Author/s:
Flanagan, DJ;Phesse, TJ;Barker, N;Schwab, RHM;Amin, N;Malaterre, J;Stange, DE;Nowell, CJ;Currie, SA;Saw, JTS;Beuchert, E;Ramsay, RG;Sansom, OJ;Ernst, M;Clevers, H;Vincan, E

Title:
Frizzled7 functions as a Wnt receptor in intestinal epithelial Lgr5+ stem cells

Date:
2015-05-12

Citation:
Flanagan, D. J., Phesse, T. J., Barker, N., Schwab, R. H. M., Amin, N., Malaterre, J., Stange, D. E., Nowell, C. J., Currie, S. A., Saw, J. T. S., Beuchert, E., Ramsay, R. G., Sansom, O. J., Ernst, M., Clevers, H. & Vincan, E. (2015). Frizzled7 functions as a Wnt receptor in intestinal epithelial Lgr5+ stem cells. Stem Cell Reports, 4 (5), pp.759-767. https://doi.org/10.1016/j.stemcr.2015.03.003.

Persistent Link:
https://hdl.handle.net/11343/210779

Stem Cell Reports
Report
OPEN ACCESS

Frizzled7 Functions as a Wnt Receptor in Intestinal Epithelial Lgr5$^+$ Stem Cells

Dustin J. Flanagan,[1,2,10] Toby J. Phesse,[3,10,11] Nick Barker,[4,5,10] Renate H.M. Schwab,[1,2] Nancy Amin,[1,2] Jordane Malaterre,[6] Daniel E. Stange,[7] Cameron J. Nowell,[3] Scott A. Currie,[1,2] Jarel T.S. Saw,[1,2] Eva Beuchert,[1,2] Robert G. Ramsay,[6] Owen J. Sansom,[8] Matthias Ernst,[3,11] Hans Clevers,[7] and Elizabeth Vincan[1,2,9,*]

[1]Department of Anatomy and Neuroscience, University of Melbourne, Melbourne, VIC 3010, Australia
[2]Victorian Infectious Diseases Reference Laboratory, Melbourne, VIC 3000, Australia
[3]Walter and Eliza Hall Institute and Department of Medical Biology, University of Melbourne, Melbourne, VIC 3010, Australia
[4]Institute of Medical Biology, Singapore 138648, Singapore
[5]MRC Centre for Regenerative Medicine, University of Edinburgh, Edinburgh EH8 9YL, UK
[6]Sir Peter MacCallum Department of Oncology, University of Melbourne, Melbourne, VIC 3010, Australia
[7]Hubrecht Institute for Developmental Biology and Stem Cell Research, 3584CT Utrecht, the Netherlands
[8]Cancer Research UK Beatson Institute, Glasgow G61 1BD, UK
[9]Curtin University, Perth, WA 6845, Australia
[10]Co-first author
[11]Present address: Olivia Newton-John Cancer Research Institute, Heidelberg, VIC 3084, Australia
*Correspondence: evincan@unimelb.edu.au
http://dx.doi.org/10.1016/j.stemcr.2015.03.003

SUMMARY

The mammalian adult small intestinal epithelium is a rapidly self-renewing tissue that is maintained by a pool of cycling stem cells intermingled with Paneth cells at the base of crypts. These crypt base stem cells exclusively express Lgr5 and require Wnt3 or, in its absence, Wnt2b. However, the Frizzled (Fzd) receptor that transmits these Wnt signals is unknown. We determined the expression profile of *Fzd* receptors in Lgr5$^+$ stem cells, their immediate daughter cells, and Paneth cells. Here we show *Fzd7* is enriched in Lgr5$^+$ stem cells and binds Wnt3 and Wnt2b. Conditional deletion of the *Fzd7* gene in adult intestinal epithelium leads to stem cell loss in vivo and organoid death in vitro. Crypts of conventional *Fzd7* knockout mice show decreased basal Wnt signaling and impaired capacity to regenerate the epithelium following deleterious insult. These observations indicate that Fzd7 is required for robust Wnt-dependent processes in Lgr5$^+$ intestinal stem cells.

INTRODUCTION

The adult intestinal epithelium is a self-renewing tissue with a high turnover rate maintained by intestinal stem cells that reside at the base of glands (called crypts). Lgr5 (leucine-rich-repeat-containing G protein-coupled receptor 5), a Wnt/β-catenin target gene, exclusively marks these long-lived crypt-based columnar (CBC) stem cells in the mouse and human intestine (Barker, 2014; Barker et al., 2007; Itzkovitz et al., 2012). Wnt/β-catenin signaling is crucial for normal stem cell function in the intestinal epithelium (Korinek et al., 1998; Sato et al., 2009). More specifically, Wnt3 signaling, provided by flanking Paneth cells, is necessary for the maintenance and function of CBC stem cells (Sato et al., 2011). In the absence of Wnt3, Wnt2b can compensate (Farin et al., 2012). The weak short range Wnt signal is augmented by R-spondin signaling through Lgr receptors (Carmon et al., 2011; de Lau et al., 2011). R-spondins are incorporated into a complex that contains Lrp (low-density lipoprotein receptor-related proteins), Lgr, and Fzd (Frizzled); this complex facilitates Fzd-coupled Wnt/β-catenin signaling. Although studies show that Wnt is critical for stem cell function (Farin et al., 2012; Sato et al., 2011), other studies question the requirement for secreted Wnt and the source of Wnt in vivo (for example, San Roman et al., 2014). Here we circumvent these controversies by investigating Fzd function.

Of the ten mammalian Fzds, only Fzd7 is frequently upregulated in stem cell populations and cancers from diverse tissues (Vincan and Barker, 2008). Cell fractionation (Mariadason et al., 2005) and in situ mRNA expression (Gregorieff et al., 2005) studies show that *Fzd7* is at the base of intestinal crypts, the correct location to transmit stem cell Wnt signals. Using tissue- and cell-specific gene deletion, we demonstrate that Wnt-dependent Lgr5$^+$ stem cell processes are impaired in the absence of Fzd7.

RESULTS

Fzd7 Expression Is Enriched in the Lgr5$^+$ Stem Cells

First, we determined the expression profile of Fzd receptors along the crypt axis using our gene array data (Agilent) (Muñoz et al., 2012). We used the *Lgr5$^{EGFP\text{-}IRES\text{-}CreERT2}$* knockin mouse (*Lgr5Cre^{ERT2}* for simplicity) where expression of EGFP is under the control of the *Lgr5* promoter (Figure 1A) (Barker et al., 2007). Isolated small intestine crypt cells were analyzed by fluorescence-activated cell sorting (FACS) and arbitrarily sorted into five fractions based on

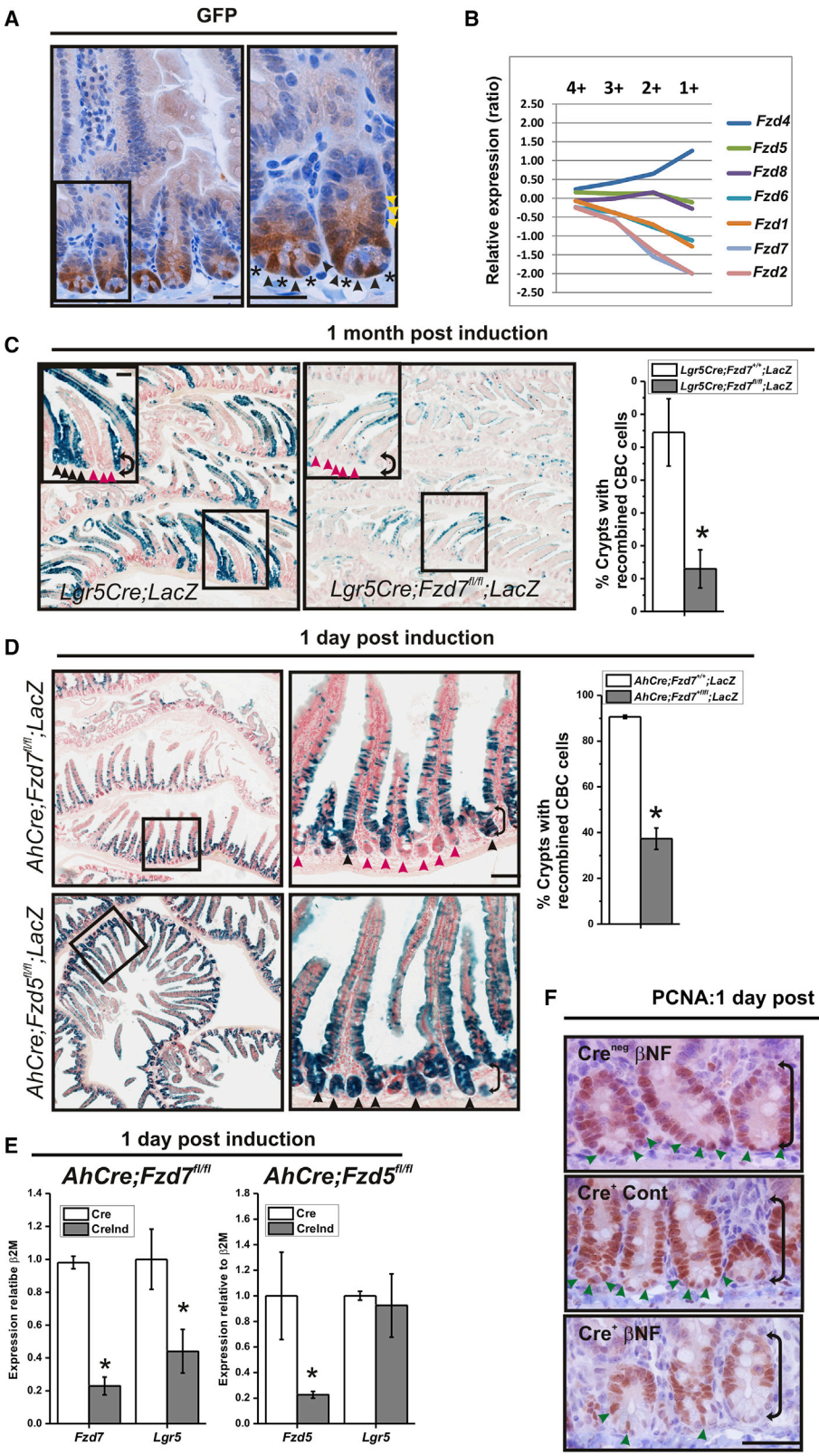

(legend on next page)

EGFP intensity. The half-life of EGFP is relatively long; thus, the level of EGFP protein is diluted as the cells divide segregating the cells along the crypt axis from CBC cell (5+, highest EGFP) to dim daughter cells (1+). As expected, expression levels of *Lgr5* rapidly decreased along the crypt axis away from the base (Muñoz et al., 2012). Similarly, the *Fzd* gene profile of each fraction was compared with fraction 5+. *Fzd2* and *Fzd7* tracked together, with highest relative expression in the CBC stem cells and then decreasing along the crypt axis away from the base. Expression of some *Fzds* did not change (*Fzd5* and *Fzd8*), whereas others (*Fzd4*) increased in cells with the least EGFP (Figure 1B). Independent FACS sorting into bulk EGFP^{+} and EGFP^{neg} populations and qRT-PCR expression analysis confirmed that *Fzd2/7* expression was enriched to the EGFP^{+} fraction, which primarily contains the *Lgr5*$^{+}$ (qRT-PCR) CBC cells (Figure S1A). Mining our gene array analysis (Affymetrix) (Muñoz et al., 2012) of CBC stem cells (EGFP^{hi}) compared with dim daughter cells (EGFP^{low}) identified high relative expression of *Fzd2* and *Fzd7* in CBC stem cells (Figure S1B), while our comparison of CBC and Paneth cells (Sato et al., 2011) showed *Fzd9* highest in the Paneth cells (Figure S1C).

Fzd7 Gene-Deleted CBC Cells Are Lost from the Epithelium

To investigate the function of *Fzd7* in adult Lgr5^{+} intestinal stem cells, we generated floxed *Fzd7* mice (*Fzd7*$^{fl/fl}$) where the Fzd7 coding region was flanked by *LoxP* sites (Figures S1D–S1F). We then intercrossed *Fzd7*$^{fl/fl}$ with *Lgr5Cre*^{ERT2} mice to enable deletion of *Fzd7* in Lgr5^{+} intestinal stem cells. By also co-expressing the *ROSA26 LacZ* reporter, recombined cells can be tracked and detected histologically by detecting β-galactosidase activity (blue stain). When adult *Lgr5Cre*^{ERT2}*;LacZ* mice were subjected to a tamoxifen pulse, recombined (blue) crypt cells were seen at 12 hr post-induction and subsequently were proven to be the intestinal stem cells as the entire crypt-villus axis derived from the recombined stem cell stained blue, forming a continuous blue ribbon (Barker et al., 2007). Consistent with this, we observe multiple recombined crypt/villus units in the small intestine one month post-induction with tamoxifen. In stark contrast, there were markedly decreased blue ribbons or blue crypts in the intestinal epithelium of induced *Lgr5Cre*^{ERT2}*;Fzd7*$^{fl/fl}$*;LacZ* mice (Figures 1C and S2A). This indicates that recombined (blue), *Fzd7*-deleted CBC stem cells were lost from the epithelium.

The marked reduction of recombined CBC stem cells following *Fzd7* deletion suggests that loss of Fzd7 was deleterious to the CBC stem cells per se. Although all the intestinal crypts harbor Lgr5^{+} CBC stem cells in the *Lgr5Cre*^{ERT2} mice, not all Lgr5^{+} cells express EGFP or Cre activity (Barker et al., 2007; Figures 1C and S2A), making detailed molecular analysis difficult. Therefore, we next employed *AhCre* recombinase, which results in robust recombination in the intestinal epithelium, targeting all cell types except the Paneth cells (Ireland et al., 2004; van der Flier et al., 2009; Figure S2B). One day after β-naphthoflavone (βNF) induction of *AhCre;LacZ* mice (Figure S2E) or another floxed *Fzd* compound mouse, *AhCre;Fzd5*$^{fl/fl}$*;LacZ* (Figure 1D), recombined blue cells were seen in the villi and crypts, including the stem cells. However, blue, recombined cells were absent from the base of the crypts when *Fzd7* was deleted in βNF-induced *AhCre;Fzd7*$^{fl/fl}$*;LacZ* mice (Figures

Figure 1. Fzd Expression in the Intestinal Epithelium

(A) Immunohistochemical analysis of EGFP expression in the intestinal epithelium of *Lgr5*$^{EGFP\text{-}IRES\text{-}CreERT2}$ showing highest expression in the CBC (black arrowheads) between the Paneth cells (*) and decreasing gradient to dim daughter cells (yellow arrowheads). Scale bar represents 50 μm.

(B) Crypt cells isolated from *Lgr5*$^{EGFP\text{-}IRES\text{-}CreERT2}$ mice were arbitrarily sorted into five populations (5+ highest to 1+ lowest EGFP expression). *Fzd* expression (Agilent array) in each sorted population was compared with the 5+ (CBC) fraction.

(C) Histological analysis of LacZ activity showing recombined (black arrowheads) and non-recombined (red arrowheads) crypt-villi in the intestinal epithelium of *Lgr5Cre;LacZ* and *Lgr5Cre;Fzd7*$^{fl/fl}$*;LacZ* mice at 1 month post-induction. The number of crypts with recombined CBC cells was scored and is shown as a percentage of total crypts counted (mean ± SEM, *p < 0.05, n = 4 mice). Bracket indicates crypt domain. Scale bar represents 100 μm.

(D) Representative histological images of LacZ activity showing crypts with recombined (black arrowheads) and non-recombined (red arrowheads) CBC cells in intestinal crypts of *AhCre;Fzd5*$^{fl/fl}$*;LacZ* and *AhCre;Fzd7*$^{fl/fl}$*;LacZ* mice at 1 day post-induction. The number of crypts with recombined CBC cells was scored and shown as a percentage of total crypts counted (mean ± SEM, *p < 0.05, n = 4 mice). Bracket indicates crypt domain. Scale bar represents 100 μm.

(E) Gene expression (qRT-PCR) analysis on crypts isolated from *AhCre;Fzd7*$^{fl/fl}$*;LacZ* or *AhCre;Fzd5*$^{fl/fl}$*;LacZ* mice at 1 day post-induction (CreInd) compared with controls (Cre) (mean ± SEM, *p < 0.05, n = 3 mice).

(F) Immunohistochemical analysis of PCNA expression to detect cycling cells (green arrowheads) and enumeration of the number of cycling cells located between Paneth cells in the intestinal crypts of induced *AhCre;Fzd7*$^{fl/fl}$*;LacZ* (Cre^{+} βNF) and *Fzd7*$^{fl/fl}$*;LacZ* (Cre neg βNF) and non-induced *AhCre;Fzd7*$^{fl/fl}$*;LacZ* (Cre^{+} Cont) mice (mean ± SEM, *p < 0.05, n = 3 mice). Bracket indicates crypt domain. Scale bar represents 50 μm.

See also Figures S1 and S2.

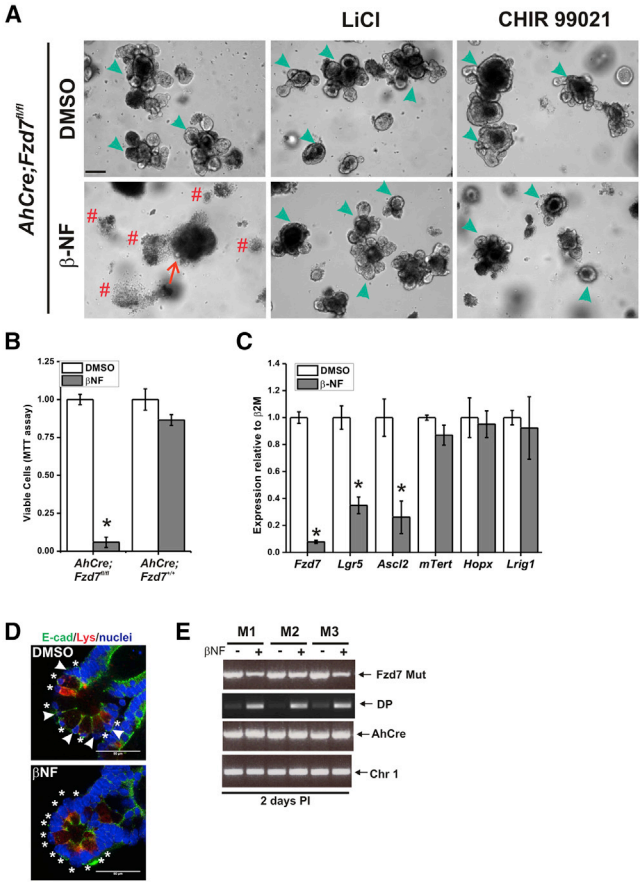

Figure 2. Fzd7 Is Required for Maintenance of Organoids

(A) Representative differential interference contrast (DIC) images of intestinal organoids from *AhCreFzd7*$^{fl/fl}$ mice showing crypt atrophy (arrow) and organoid death (#) after treatment with βNF; and rescue with LiCl or CHIR99021 added 1 day after βNF; green arrowheads indicate examples of healthy organoids. Scale bar represents 100 μm.

(B) MTT cell viability assay 3 days after passage of vehicle (DMSO) and induced (βNF-treated) organoids (mean ± SEM, *$p < 0.05$, $n = 3$ mice).

(C) Gene expression (qRT-PCR) analysis of organoids at 2 days post-induction (βNF) compared with controls (DMSO) (mean ± SEM, *$p < 0.05$, $n = 3$ mice).

(D) Immunofluorescence analysis of E-cadherin (green) and Lysozyme (red) expression in induced (βNF) and control (DMSO) organoid crypts of *AhCreFzd7*$^{fl/fl}$ mice showing Paneth cell (*) and CBC (arrowheads) positioning (nuclei blue, DAPI). Scale bar represents 50 μm.

(E) PCRs to detect the *Fzd7* mutant knockin allele (Fzd7 Mut) and recombined product after *Fzd7* gene deletion (DP), *AhCre* transgene (AhCre), and a region of chromosome 1 close to Fzd7 locus (Chr1), in genomic DNA extracted from organoids established from three *AhCreFzd7*$^{fl/fl}$ mice (M1, M2, M3) at 2 days post-induction (PI).

See also Figure S3.

1D and S2E). Molecular analysis by qRT-PCR of crypts isolated from these mice identified that *Lgr5* expression was decreased in the crypts isolated from the *Fzd7*-deleted mice, but not from the *Fzd5*-deleted mice (Figure 1E). This indicates that the CBC cells were lost after *Fzd7* deletion, but not after *Fzd5* deletion. βNF treatment alone did not result in changes in *Fzd7* or *Lgr5* expression (Figure S2C).

The base of the crypts contain Lgr5$^+$ CBC stem cells, which are highly proliferative, juxtaposed by non-proliferating Paneth cells (Barker et al., 2007; Figure 1A). Thus, to further investigate whether deletion of *Fzd7* had led to loss of CBC cells, immunohistochemistry was performed for the proliferation marker proliferating cell nuclear antigen (PCNA), and the number of proliferating cells counted. The number of proliferating cells (PCNA$^+$ nuclei) between the Paneth cells was significantly reduced in *Fzd7*-deleted crypts, further supporting the model in which *Fzd7* deletion results in loss of CBC cells (Figure 1F). Cryptidin in situ to detect Paneth cells also revealed that the Paneth cells were packed side by side without intermingled, unstained CBC cells in the crypts of *Fzd7* deleted mice. Enumeration of unstained cells between Paneth cells on the cryptidin stained sections demonstrates a significant reduction in CBC cells following *Fzd7* deletion (Figure S2F).

As the recombined CBC stem cells were lost from the epithelium of induced *AhCre;Fzd7*$^{fl/fl}$*;LacZ* mice, the blue cells were progressively "washed" off from the epithelium through normal turnover. Thus, by 4 days post-induction, the recombined cells had migrated up the crypt-villus axis, and by day 7, recombined cells had been cleared from the epithelium. Some escaper crypt-villi ribbons (blue) were seen at days 4 and 7 (Figure S2E). By day 7, *Lgr5* expression had returned to WT levels, while *Fzd7* expression was increasing (Figure S2D). These observations are consistent with a loss of recombined *Fzd7*-deleted CBC stem cells from the crypts of induced *AhCre;Fzd7*$^{fl/fl}$*;LacZ* mice.

Fzd7 Deleted Intestinal Organoids Do Not Regenerate

The loss of intestinal CBCs when *Fzd7* was deleted in vivo was transient because of the repopulation that this deleterious event triggers. To further investigate this loss of CBC following *Fzd7* gene deletion, we established organoid cultures from crypts isolated from the proximal small intestine of *AhCre;Fzd7*$^{fl/fl}$ mice and induced Cre-mediated recombination under defined conditions in vitro. Isolated crypts cultured in vitro with growth factors form mini-gut organoids with characteristics of the intact epithelium (Sato et al., 2009). Induction of *Fzd7* gene deletion (*Fzd7*$^{\Delta/\Delta}$) led to atrophy of the crypts and organoid death (Figures 2A, S3A, and S3B). Treatment of the organoids 1 day post-induction with 10-mM LiCl (Klein and Melton, 1996) or 5-μM CHIR99021 (Bennett et al., 2002) to activate

Wnt/β-catenin signaling downstream of Wnt/Fzd rescued this phenotype (Figure 2A). The *Fzd7*$^{\Delta/\Delta}$ organoids failed to regenerate upon passage, suggesting that Fzd7 is required for the maintenance and regeneration of new organoids (Figures 2B and S3D). Reduction of *Fzd7* expression in the βNF-treated cultures was confirmed by qRT-PCR (Figures 2C and S3C). The concomitant decrease in *Lgr5* expression (Figure 2C) indicated loss of CBC stem cells. Achaete-Scute homolog 2 (*Ascl2*), a transcription factor that is essential for the maintenance of Lgr5^{+} stem cells (van der Flier et al., 2009), was also decreased in the βNF-treated cultures. While, in contrast, markers of other putative intestinal stem cells (Barker, 2014) were unchanged or below detection limits (telomerase reverse transcriptase [*mTert*], homeodomain-only [*Hopx*], and leucine-rich repeats and immunoglobulin-like domains protein 1 [*Lrig1*]; Figure 2C).

Immunofluorescence analysis of the organoids revealed that the slender CBC cells were absent in the βNF-treated organoids (Figure 2D). Notably, a more marked reduction of CBCs was observed when *Fzd7* was deleted in organoids compared with deletion in vivo (Figures 1F and S2F), which indicates that there was no overlapping repopulation event occurring in the organoids. To detect recombination, we performed two PCRs on genomic DNA from organoids 2 days after βNF treatment. First, we observed excision of the mutant *Fzd7* allele (Fzd7 Mut PCR), which was partial as recombination does not occur in Paneth cells (Ireland et al., 2004; van der Flier et al., 2009; Figure S2B). Second, PCR to detect the intact genomic DNA after gene excision (DP PCR) illustrated efficient recombination in the induced mice (Figure 2E). Cultured intestinal organoids from *AhCre;Fzd7*$^{+/+}$ mice (Figures 2B and S3E) and *AhCre;Fzd5*$^{fl/fl}$ (Figure S3F) continued to grow and regenerate unimpeded following βNF treatment. Organoid death was also observed when *Fzd7* was deleted from organoids using a different Cre enzyme (*VillinCre*^{ERT2}) that targets the intestinal epithelium (el Marjou et al., 2004) (Figures S3G–S3I).

Intestinal Epithelium Regeneration Is Impaired in *Fzd7* Knockout Mice

Collectively, these data show conditional deletion of the *Fzd7* gene was deleterious to CBC stem cells in vivo and in vitro. The consequence of this deleterious insult was CBC stem cell loss in vivo and organoid death in vitro. Likewise, the intestinal crypts of conventional *Fzd7* knockout mice (*Fzd7*$^{NLS/NLS}$) showed impaired stem cell function. The *Fzd7*$^{NLS/NLS}$ are viable and fertile with no overt intestinal phenotype under basal, non-challenge conditions (Yu et al., 2012) (Figures 3A and S4A). However, careful molecular analysis by immunohistochemistry and qRT-PCR revealed that c-Myc expression was reduced in crypts isolated from *Fzd7*$^{NLS/NLS}$ mice when compared with WT mice (Figures 3C and S4B). This indicates a modest decrease in basal Wnt/β-catenin signaling as c-Myc is the main effector of active Wnt/β-catenin signaling in the crypt (Sansom et al., 2007).

This impaired signaling was exacerbated upon injury challenge to the epithelium. In the mouse intestine, tissue injury can be experimentally stimulated by whole-body exposure to ionizing radiation. After a whole-body single 14-Gy dose, the intestinal crypt cells die by apoptosis, and subsequently, the tissue is denuded by 48 hr post-irradiation. This triggers rapid repopulation by stem cells and massive expansion of the crypt compartment (Ashton et al., 2010). Consistent with this, we observed ablation of the crypts at 48h and regeneration at 70 hr in WT mice. However, regeneration was dramatically impaired in the *Fzd7*$^{NLS/NLS}$ mice with significantly fewer regenerating crypts scored per intestinal cross-section at 70h when compared with WT (Figure 3A). *c-Myc* and several other TCF/β-catenin transcriptional target genes known to be upregulated during regeneration (Ashton et al., 2010) were decreased in *Fzd7*$^{NLS/NLS}$ crypts compared with WT mice at this time point (Figure 3B). This failure of *Fzd7*$^{NLS/NLS}$ mice to upregulate c-Myc after irradiation was confirmed by immunohistochemistry (Figure 3C). Regeneration was observed in the *Fzd7*$^{NLS/NLS}$ mice at 120 hr post-irradiation, suggesting that loss of Fzd7 delays, rather than prevents, intestinal regeneration (Figure 3A). Thus, Fzd7 is required for efficient, robust regeneration of the intestinal epithelium, a process that requires high levels of Wnt/β-catenin signaling (Ashton et al., 2010) and is documented to be absolutely dependent on Lgr5^{+} stem cells (Metcalfe et al., 2014).

Closely Related *Fzd* Genes Cannot Compensate for *Fzd7* Loss

Fzd1, *Fzd2*, and *Fzd7* form a subclass of *Fzd* genes that share strong sequence identity in the intracellular C-terminal domain and can potentially play redundant roles (Sagara et al., 1998; Yu et al., 2012). qRT-PCR was performed on cDNA derived from crypts isolated from irradiated WT mice, demonstrating that *Fzd7*, but not *Fzd1* or *Fzd2*, was upregulated during regeneration (Figure 4A). However, *Fzd1* and *Fzd2* were upregulated in the regenerating epithelium of *Fzd7*$^{NLS/NLS}$ mice (Figure 4B), but presumably, this upregulation was insufficient to promote intestinal regeneration as regeneration was impaired in these mice (Figure 3) despite a 2-fold increase in *Lgr5* expression (Figure 4C). Consistent with the observed delayed regeneration and absence of cycling (PCNA^{+}) cells in the *Fzd7*$^{NLS/NLS}$ mice at 70 hr post-irradiation, expression of P21, the potent cyclin-kinase-dependent inhibitor, was elevated when compared with WT mice (Figures 4C and 4D).

Collectively, these data demonstrate that Fzd7-mediated Wnt/β-catenin signaling is necessary for optimal

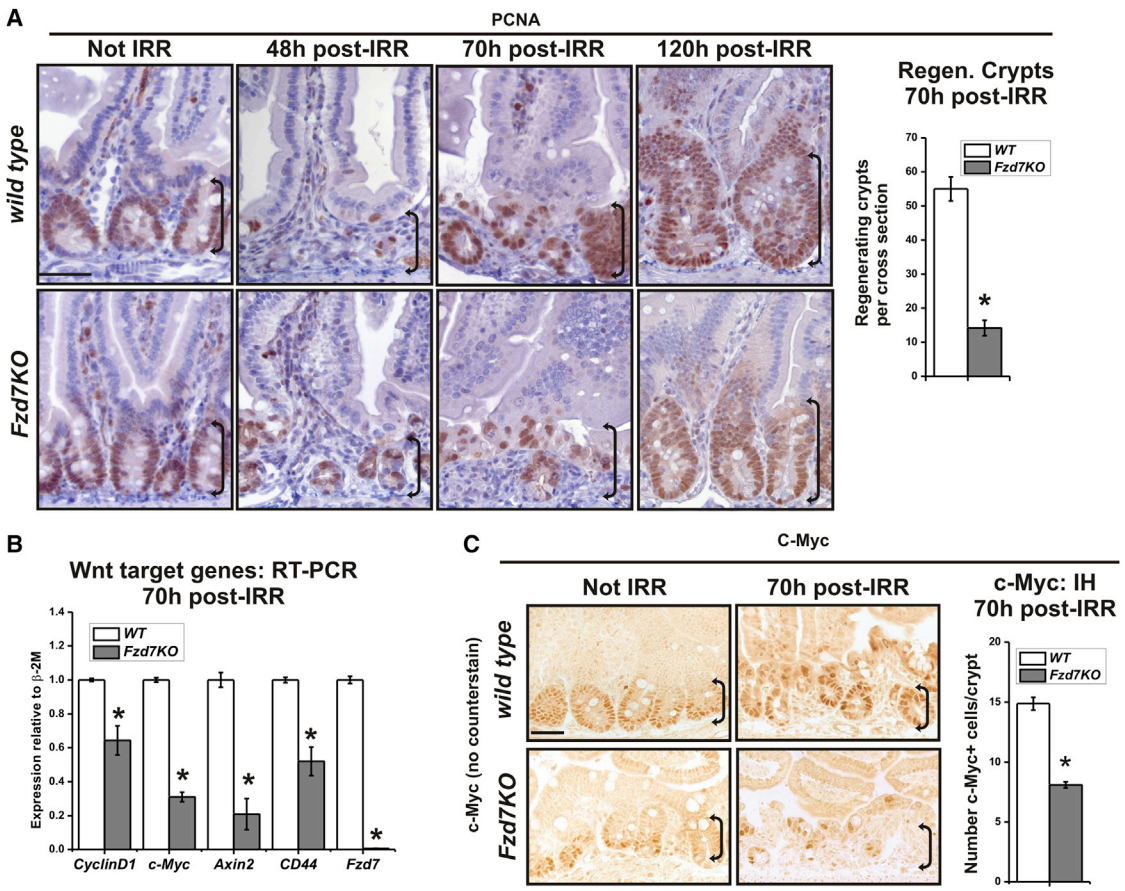

Figure 3. Impaired Intestine Epithelium Regeneration in Fzd7 KO Mice

(A) Immunohistochemical analysis of PCNA expression (cycling cells) in the small intestine epithelium of non-irradiated (not IRR) mice and at indicated times post-irradiation (post-IRR). Brackets indicate crypt domain. Efficiency of regeneration was quantified by counting the number of regenerating crypts per intestine cross-section at 70 hr post-IRR (mean ± SEM, *$p < 0.05$, $n \geq 5$ mice). Scale bar represents 50 μm.

(B) Wnt target gene expression (qRT-PCR) in isolated intestinal crypts 70 hr post-IRR (mean ± SEM, *$p < 0.05$, $n = 6$ mice).

(C) Immunohistochemical analysis of c-MYC expression (no hematoxylin counterstain) in the intestinal epithelium at 70 hr post-IRR and the enumeration of nuclear c-MYC$^+$ cells per crypt at 70 hr post-IRR (mean ± SEM, *$p < 0.05$, $n = 4$ mice). Scale bar represents 50 μm.

See also Figures S4A and S4B.

regeneration of the intestinal epithelium. Wnt3 (Sato et al., 2011) or Wnt2b (Farin et al., 2012) are required for intestinal stem cell function. FZD7 has been reported as a receptor for WNT3 (Kim et al., 2008). Here we confirmed interaction between FZD7 and WNT3 by co-immunoprecipitation of epitope tagged FZD7 and WNT3 proteins in HEK293T cells and extended this to show FZD7 also binds WNT2b (Figures 4E and S4C).

DISCUSSION

Taken together, our data show that Fzd7, at least in part, transmits the critical Wnt signal in intestinal CBC stem cells. Expression of *Fzd7* was enriched in Lgr5$^+$ stem cells, and Fzd7 signaling was necessary for competent Lgr5$^+$ stem cell function, as in the absence of Fzd7, crypt homeostasis and epithelium regeneration were compromised. Closely related Fzds could not fully compensate for Fzd7 loss.

We observed a rapid loss of CBC cells 1 day after *Fzd7* deletion in induced *AhCre;Fzd7$^{fl/fl}$* mice. By counting PCNA$^+$ cells between the Paneth cells or unstained CBC cells between cryptidin stained Paneth cells, as surrogate markers for CBCs, we avoid the documented pitfalls of stem cell marker specificity (Barker, 2014; Itzkovitz et al., 2012; Metcalfe et al., 2014). Recombination using with *Lgr5Cre^{ERT2}* mice confirmed that deletion of *Fzd7*

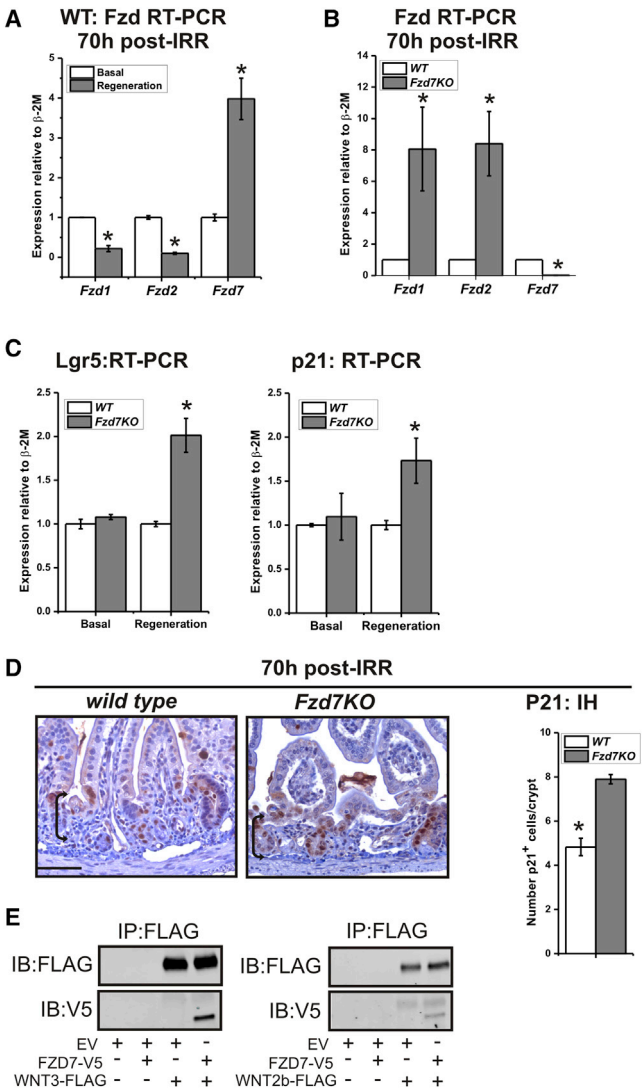

Figure 4. Closely Related Fzds Cannot Compensate for Fzd7 Loss

(A) *Fzd* expression (qRT-PCR) in basal and regenerating (70 hr post-IRR) intestinal crypts of WT mice (mean ± SEM, *p < 0.05, n = 4 mice).

(B) *Fzd* expression (qRT-PCR) in WT and $Fzd7^{NLS/NLS}$ (Fzd7KO) regenerating (70 hr post-IRR) intestinal crypts (mean ± SEM, *p < 0.05, n = 4 mice).

(C) *Lgr5* and *p21* expression (qRT-PCR) in basal and regenerating (70 hr post-IRR) intestinal epithelium crypts (mean ± SEM, *p < 0.05, n = 4 mice).

(D) Immunohistochemical analysis of P21 expression in WT and $Fzd7^{NLS/NLS}$ (Fzd7KO) regenerating (70 hr post-IRR) intestinal crypts. Brackets indicate crypt domain and the enumeration of $P21^+$ cells per crypt at 70 hr post-IRR (mean ± SEM, *p < 0.05, n = 4 mice). Scale bar represents 50 μm.

(E) Immunoblot (IB) of FLAG immunoprecipitates (IP) from HEK293T cells transfected with the indicated expression plasmids. See also Figure S4C.

specifically in $Lgr5^+$ cells was deleterious to these intestinal stem cells. Similar rapid loss of stem cells following deleterious gene deletions was observed previously with c-Myc (Muncan et al., 2006) and Ascl2 (van der Flier et al., 2009), for example. The epithelium recovers rapidly from these deleterious insults in vivo. Two mechanisms have been described recently to account for the rapid repopulation with stem cells: dedifferentiation of partially committed progenitors of the secretory cell lineages (Basak et al., 2014; Buczacki et al., 2013; van Es et al., 2012) or triggering mature quiescent Paneth cells to reacquire stem cell properties in situations of damage and repair (Roth et al., 2012). Either mechanism could account for repopulation in our experiments.

Notably, FZD7 plays a non-redundant role in maintaining pluripotency of human embryonic stem cells (Fernandez et al., 2014) and might play a similar role in the intestinal stem cells. Our study demonstrates that intestinal stem cells that do not express Fzd7 have an inherent defect in Wnt/β-catenin signaling, which compromises stem cell function under conditions of stress. Fzd7 therefore might provide an avenue to specifically manipulate Wnt-driven processes in intestinal stem cells.

EXPERIMENTAL PROCEDURES

Mice

The $Lgr5^{EGFP\text{-}Ires\text{-}CreERT2}$ (Barker et al., 2007), *AhCre* (Ireland et al., 2004), $Fzd5^{fl/fl}$ (van Es et al., 2005) and $Fzd7^{NLS}$ (Yu et al., 2012) were interbred to generate compound mice with appropriate alleles. All mice were co-housed, and with the exception of $Fzd7^{NLS}$, all mice were on an inbred C57BL/6 genetic background using appropriate littermates as controls. The $Fzd7^{NLS}$ were on a mixed C57BL/6 × Sv129 background. For regeneration studies, adult mice were irradiated as described previously (Phesse et al., 2014). Briefly, mice were exposed to a single 14-Gy dose of whole-body γ irradiation and harvested at the time points indicated. All animal experiments were approved by the Animal Ethics Committee, Office for Research Ethics and Integrity, University of Melbourne.

Cre Induction and Analyses of Mouse Tissues

Mice aged 6–12 weeks were given on the same day two 200-μl intraperitoneal injections of tamoxifen in sunflower oil at 10 mg/ml or three 200-μl intraperitoneal injections of βNF in corn oil at 10 mg/ml. Tissues were harvested at the indicated times after the first dose. So that the pattern of Cre-mediated recombination at the *ROSA26R LacZ* reporter locus could be determined, intestines were stained for the presence of β-galactosidase (LacZ) activity (see the Supplemental Experimental Procedures). Immunohistochemistry and in situ hybridization was performed on formalin-fixed paraffin-embedded tissue sections. Rabbit primary antibodies used were anti-GFP (Invitrogen, AG455) and anti-PCNA, anti-c-Myc, and anti-P21 (Santa Cruz SC7907, SC764, and SC397, respectively). Detection of antibody binding was with the rabbit Impress

kit (Vector, MP7401). Unless otherwise stated, slides were counterstained with hematoxylin. Original magnification of images was ×200 or ×400. FACS sorting and gene expression analyses using Affymetrix and Agilent arrays have been described in detail previously (Muñoz et al., 2012; Sato et al., 2011) (also see the Supplemental Experimental Procedures).

Crypt Organoid Culture and Analysis

Crypt isolation and organoid culture was performed by modified previously described protocols (Sato et al., 2009). Crypt isolation, immunofluorescence staining, 3-[4,5-dimethylthiazol-2-yl]-2,5-diphenyl tetrazolium bromide (MTT) cell viability assay, and qRT-PCR are detailed in the Supplemental Experimental Procedures. The primary antibodies were mouse anti-E cadherin (BD Transduction labs, 610181) and rabbit anti-lysozyme (Thermo Scientific, RB372); the secondary antibodies were Alexa anti mouse568 and Alexa anti rabbit 488.

Co-immunopreciptation and Immunoblot Analysis

HEK293 cells were co-transfected with FZD7 ectodomain-V5 and FLAG tagged WNT3 or WNT2b. FLAG IP was performed using the Anti-FLAG M2 Affinity Gel kit (Sigma) (also see the Supplemental Experimental Procedures).

Statistical Analysis

Data are expressed as mean ± SEM, where mean represents number of mice (three or more per genotype) or number of experiments (three or more). Unless stated otherwise, organoids were established from three or more hosts per group. Statistical tests used are Student's t test or Mann-Whitney with Prism5 (GraphPad software) where p values of ≤ 0.05 were considered significant.

SUPPLEMENTAL INFORMATION

Supplemental Information includes Supplemental Experimental Procedures and four figures and can be found with this article online at http://dx.doi.org/10.1016/j.stemcr.2015.03.003.

AUTHOR CONTRIBUTIONS

E.V. and N.B. conceived the study. E.V., T.J.P., N.B., and H.C. designed aspects of the study. D.J.F., R.H.M.S., N.A., J.M., D.E.S., S.A.C., J.T.S.S., E.B., E.V., and N.B. performed experiments. T.J.P., R.G.R., O.J.S., M.E., H.C., and E.V. supervised specific experiments. C.J.N. provided imaging analysis. E.V., T.J.P., N.B., and H.C. analyzed and interpreted data. E.V., T.J.P., and N.B. wrote the paper.

ACKNOWLEDGMENTS

We thank D.L. Neate and B.M. Tran for technical assistance. We thank A.R. Clarke for the AhCre mice and C.D. Mao for the expression plasmids. This work was supported by grants from NHMRC #566679 (E.V., N.B., H.C.), #603127 and #1025239 (T.J.P.), #1079257 (M.E.), and #487922 (M.E. and R.G.R.); Melbourne Health #605030 (E.V., N.B., T.J.P., H.C.), and the Cancer Council of Victoria (CCV) #APP1020716 (E.V., N.B., T.J.P., H.C.); and post-graduate awards from the CCV (D.J.F.) and Melbourne Health (R.H.M.S.). M.E. and R.G.R. are NHMRC Senior Research Fellows.

Received: September 13, 2014
Revised: March 18, 2015
Accepted: March 20, 2015
Published: April 16, 2015

REFERENCES

Ashton, G.H., Morton, J.P., Myant, K., Phesse, T.J., Ridgway, R.A., Marsh, V., Wilkins, J.A., Athineos, D., Muncan, V., Kemp, R., et al. (2010). Focal adhesion kinase is required for intestinal regeneration and tumorigenesis downstream of Wnt/c-Myc signaling. Dev. Cell *19*, 259–269.

Barker, N. (2014). Adult intestinal stem cells: critical drivers of epithelial homeostasis and regeneration. Nat. Rev. Mol. Cell Biol. *15*, 19–33.

Barker, N., van Es, J.H., Kuipers, J., Kujala, P., van den Born, M., Cozijnsen, M., Haegebarth, A., Korving, J., Begthel, H., Peters, P.J., and Clevers, H. (2007). Identification of stem cells in small intestine and colon by marker gene Lgr5. Nature *449*, 1003–1007.

Basak, O., van de Born, M., Korving, J., Beumer, J., van der Elst, S., van Es, J.H., and Clevers, H. (2014). Mapping early fate determination in Lgr5+ crypt stem cells using a novel Ki67-RFP allele. EMBO J. *33*, 2057–2068.

Bennett, C.N., Ross, S.E., Longo, K.A., Bajnok, L., Hemati, N., Johnson, K.W., Harrison, S.D., and MacDougald, O.A. (2002). Regulation of Wnt signaling during adipogenesis. J. Biol. Chem. *277*, 30998–31004.

Buczacki, S.J., Zecchini, H.I., Nicholson, A.M., Russell, R., Vermeulen, L., Kemp, R., and Winton, D.J. (2013). Intestinal label-retaining cells are secretory precursors expressing Lgr5. Nature *495*, 65–69.

Carmon, K.S., Gong, X., Lin, Q., Thomas, A., and Liu, Q. (2011). R-spondins function as ligands of the orphan receptors LGR4 and LGR5 to regulate Wnt/beta-catenin signaling. Proc. Natl. Acad. Sci. USA *108*, 11452–11457.

de Lau, W., Barker, N., Low, T.Y., Koo, B.K., Li, V.S., Teunissen, H., Kujala, P., Haegebarth, A., Peters, P.J., van de Wetering, M., et al. (2011). Lgr5 homologues associate with Wnt receptors and mediate R-spondin signalling. Nature *476*, 293–297.

el Marjou, F., Janssen, K.P., Chang, B.H., Li, M., Hindie, V., Chan, L., Louvard, D., Chambon, P., Metzger, D., and Robine, S. (2004). Tissue-specific and inducible Cre-mediated recombination in the gut epithelium. Genesis *39*, 186–193.

Farin, H.F., Van Es, J.H., and Clevers, H. (2012). Redundant sources of wnt regulate intestinal stem cells and promote formation of paneth cells. Gastroenterology *143*, 1518–1529.e7.

Fernandez, A., Huggins, I.J., Perna, L., Brafman, D., Lu, D., Yao, S., Gaasterland, T., Carson, D.A., and Willert, K. (2014). The WNT receptor FZD7 is required for maintenance of the pluripotent state in human embryonic stem cells. Proc. Natl. Acad. Sci. USA *111*, 1409–1414.

Gregorieff, A., Pinto, D., Begthel, H., Destrée, O., Kielman, M., and Clevers, H. (2005). Expression pattern of Wnt signaling components in the adult intestine. Gastroenterology *129*, 626–638.

Ireland, H., Kemp, R., Houghton, C., Howard, L., Clarke, A.R., Sansom, O.J., and Winton, D.J. (2004). Inducible Cre-mediated

control of gene expression in the murine gastrointestinal tract: effect of loss of beta-catenin. Gastroenterology *126*, 1236–1246.

Itzkovitz, S., Lyubimova, A., Blat, I.C., Maynard, M., van Es, J., Lees, J., Jacks, T., Clevers, H., and van Oudenaarden, A. (2012). Single-molecule transcript counting of stem-cell markers in the mouse intestine. Nat. Cell Biol. *14*, 106–114.

Kim, M., Lee, H.C., Tsedensodnom, O., Hartley, R., Lim, Y.S., Yu, E., Merle, P., and Wands, J.R. (2008). Functional interaction between Wnt3 and Frizzled-7 leads to activation of the Wnt/beta-catenin signaling pathway in hepatocellular carcinoma cells. J. Hepatol. *48*, 780–791.

Klein, P.S., and Melton, D.A. (1996). A molecular mechanism for the effect of lithium on development. Proc. Natl. Acad. Sci. USA *93*, 8455–8459.

Korinek, V., Barker, N., Moerer, P., van Donselaar, E., Huls, G., Peters, P.J., and Clevers, H. (1998). Depletion of epithelial stem-cell compartments in the small intestine of mice lacking Tcf-4. Nat. Genet. *19*, 379–383.

Mariadason, J.M., Nicholas, C., L'Italien, K.E., Zhuang, M., Smartt, H.J., Heerdt, B.G., Yang, W., Corner, G.A., Wilson, A.J., Klampfer, L., et al. (2005). Gene expression profiling of intestinal epithelial cell maturation along the crypt-villus axis. Gastroenterology *128*, 1081–1088.

Metcalfe, C., Kljavin, N.M., Ybarra, R., and de Sauvage, F.J. (2014). Lgr5+ stem cells are indispensable for radiation-induced intestinal regeneration. Cell Stem Cell *14*, 149–159.

Muncan, V., Sansom, O.J., Tertoolen, L., Phesse, T.J., Begthel, H., Sancho, E., Cole, A.M., Gregorieff, A., de Alboran, I.M., Clevers, H., and Clarke, A.R. (2006). Rapid loss of intestinal crypts upon conditional deletion of the Wnt/Tcf-4 target gene c-Myc. Mol. Cell. Biol. *26*, 8418–8426.

Muñoz, J., Stange, D.E., Schepers, A.G., van de Wetering, M., Koo, B.K., Itzkovitz, S., Volckmann, R., Kung, K.S., Koster, J., Radulescu, S., et al. (2012). The Lgr5 intestinal stem cell signature: robust expression of proposed quiescent '+4' cell markers. EMBO J. *31*, 3079–3091.

Phesse, T.J., Buchert, M., Stuart, E., Flanagan, D.J., Faux, M., Afshar-Sterle, S., Walker, F., Zhang, H.H., Nowell, C.J., Jorissen, R., et al. (2014). Partial inhibition of gp130-Jak-Stat3 signaling prevents Wnt-β-catenin-mediated intestinal tumor growth and regeneration. Sci. Signal. *7*, ra92.

Roth, S., Franken, P., Sacchetti, A., Kremer, A., Anderson, K., Sansom, O., and Fodde, R. (2012). Paneth cells in intestinal homeostasis and tissue injury. PLoS ONE *7*, e38965.

Sagara, N., Toda, G., Hirai, M., Terada, M., and Katoh, M. (1998). Molecular cloning, differential expression, and chromosomal localization of human frizzled-1, frizzled-2, and frizzled-7. Biochem. Biophys. Res. Commun. *252*, 117–122.

San Roman, A.K., Jayewickreme, C.D., Murtaugh, L.C., and Shivdasani, R.A. (2014). Wnt secretion from epithelial cells and subepithelial myofibroblasts is not required in the mouse intestinal stem cell niche in vivo. Stem Cell Reports *2*, 127–134.

Sansom, O.J., Meniel, V.S., Muncan, V., Phesse, T.J., Wilkins, J.A., Reed, K.R., Vass, J.K., Athineos, D., Clevers, H., and Clarke, A.R. (2007). Myc deletion rescues Apc deficiency in the small intestine. Nature *446*, 676–679.

Sato, T., Vries, R.G., Snippert, H.J., van de Wetering, M., Barker, N., Stange, D.E., van Es, J.H., Abo, A., Kujala, P., Peters, P.J., and Clevers, H. (2009). Single Lgr5 stem cells build crypt-villus structures in vitro without a mesenchymal niche. Nature *459*, 262–265.

Sato, T., van Es, J.H., Snippert, H.J., Stange, D.E., Vries, R.G., van den Born, M., Barker, N., Shroyer, N.F., van de Wetering, M., and Clevers, H. (2011). Paneth cells constitute the niche for Lgr5 stem cells in intestinal crypts. Nature *469*, 415–418.

van der Flier, L.G., van Gijn, M.E., Hatzis, P., Kujala, P., Haegebarth, A., Stange, D.E., Begthel, H., van den Born, M., Guryev, V., Oving, I., et al. (2009). Transcription factor achaete scute-like 2 controls intestinal stem cell fate. Cell *136*, 903–912.

van Es, J.H., Jay, P., Gregorieff, A., van Gijn, M.E., Jonkheer, S., Hatzis, P., Thiele, A., van den Born, M., Begthel, H., Brabletz, T., et al. (2005). Wnt signalling induces maturation of Paneth cells in intestinal crypts. Nat. Cell Biol. *7*, 381–386.

van Es, J.H., Sato, T., van de Wetering, M., Lyubimova, A., Nee, A.N., Gregorieff, A., Sasaki, N., Zeinstra, L., van den Born, M., Korving, J., et al. (2012). Dll1+ secretory progenitor cells revert to stem cells upon crypt damage. Nat. Cell Biol. *14*, 1099–1104.

Vincan, E., and Barker, N. (2008). The upstream components of the Wnt signalling pathway in the dynamic EMT and MET associated with colorectal cancer progression. Clin. Exp. Metastasis *25*, 657–663.

Yu, H., Ye, X., Guo, N., and Nathans, J. (2012). Frizzled 2 and frizzled 7 function redundantly in convergent extension and closure of the ventricular septum and palate: evidence for a network of interacting genes. Development *139*, 4383–4394.